Journal of Neuroscience Methods 372 (2022) 109536

Contents lists available at ScienceDirect

Journal of Neuroscience Methods

journal homepage: www.elsevier.com/locate/jneumeth

Focused ultrasound stimulation of an *ex-vivo Aplysia* abdominal ganglion preparation

Tomas Jordan [a], James M. Newcomb [b], Michael B. Hoppa [c], Geoffrey P. Luke [a,*]

[a] Thayer School of Engineering, Dartmouth College, Hanover, NH 03755, USA
[b] Department of Biology and Health Science, New England College, Henniker, NH 03242, USA
[c] Department of Biological Sciences, Dartmouth College, Hanover, NH 03755, USA

ARTICLE INFO

Keywords:
Ultrasound neurostimulation
Focused ultrasound
Aplysia californica
Abdominal ganglion

ABSTRACT

Background: A growing body of research demonstrates that focused ultrasound stimulates activity in human and other mammalian nervous systems. However, there is no consensus on which sonication parameters are optimal. Furthermore, the mechanism of action behind ultrasound neurostimulation remains poorly understood. An invertebrate model greatly reduces biological complexity, permitting a systematic evaluation of sonication parameters suitable for ultrasound neurostimulation.

New Method: Here, we describe the use of focused ultrasound stimulation with an *ex-vivo* abdominal ganglion preparation of the California sea hare, *Aplysia californica*, a long-standing model system in neurobiology. We developed a system for stimulating an isolated ganglion preparation while obtaining extracellular recordings from nerves. The focused ultrasound stimulation uses one of two single-element transducers, enabling stimulation at four distinct carrier frequencies (0.515 MHz, 1.l MHz, 1.61 MHz, 3.41 MHz).

Results: Using continuous wave ultrasound, we stimulated the ganglion at all four frequencies, and we present quantitative evaluation of elicited activation at four different sonication durations and three peak pressure levels, eliciting up to a 57-fold increase in spiking frequency.

Comparison with Electrical Stimulation: We demonstrated that ultrasound-induced activation is repeatable, and the response consistency is comparable to electrical stimulation.

Conclusions: Due to the relative ease of long-term recordings for many hours, this *ex-vivo* ganglion preparation is suitable for investigating sonication parameters and the effects of focused ultrasound stimulation on neurons.

1. Introduction

Focused ultrasound (FUS) stimulation is emerging as an increasingly popular technique for stimulating neural activity in the central nervous system. Compared to other established methods (such as electrical stimulation, transcranial magnetic stimulation, or transcranial direct current stimulation), FUS offers several advantages particularly suitable for applications in the brain. Ultrasound can be focused into a small volume of tissue, based on the wavelength of the carrier frequency (~3 mm at 0.5 MHz, < 100 μm at frequencies higher than 40 MHz (Legon et al., 2018; Menz et al., 2013)). The energy is delivered non-invasively and the penetration depth can reach several centimeters, depending on the frequency (Chivers and Hill, 1975; Newman, 2008). Further, the temporal resolution of ultrasound stimulation greatly exceeds the maximum firing rates of neurons (Wang et al., 2016). Overall, FUS enables non-invasive activation of select regions in the brain with high spatiotemporal precision.

While it is most commonly reported that FUS stimulation increases neural activity the degree of stimulation is much more variable. Indeed, under some stimulation parameters it has been reported to detect a suppression in neural activity or firing frequency (Bachtold et al., 1998; Choi et al., 2013; Kim et al., 2017). Additionally, this inhibition of activity can be reversible or permanent, depending on the sonication duration (Fry et al., 1958). Careful selection of sonication parameters is therefore critical for achieving desired outcomes. However, there is no consensus on what parameters are optimal for efficient stimulation or inhibition of neural activity. Some research groups argue that pulsed FUS produces more reliable outcomes, while others claim that a

Abbreviations: FUS, focused ultrasound; FWHM, Full-width half maximum.

* Corresponding author.
E-mail address: Geoffrey.p.luke@dartmouth.edu (G.P. Luke).

https://doi.org/10.1016/j.jneumeth.2022.109536
Received 7 October 2021; Received in revised form 17 January 2022; Accepted 20 February 2022
Available online 25 February 2022

continuous wave is preferred (Kim et al., 2014; King et al., 2013). There is a growing body of literature reporting on ultrasound neurostimulation carried out in various animal models, at different frequencies, intensities, and sonication durations (Blackmore et al., 2019). However, many studies only investigate the effects of changing a single parameter. Further, the ultrasound carrier frequency is often held constant since studying a range of frequencies may be dependent on the availability of multiple transducers. Overall, there is a lack of comprehensive studies that investigate the effects of varying all stimulation parameters in order to identify which parameters lead to efficient activation.

It is also unclear how ultrasound stimulation causes electrical changes in neurons (Jerusalem et al., 2019). It is possible that the ultrasound-induced mechanical deformations of the membrane lead to generation of capacitive currents (Plaksin et al., 2014; Prieto et al., 2013). Alternatively, the ultrasound waves may be interacting with mechanosensitive ion channels (Brohawn, 2015; Kubanek et al., 2016). Ultrasound or resulting cavitation effects may lead to opening of pores in the lipid bilayer which could act as ion transport channels – this process is referred to as sonoporation (Haar, 2010; Krasovitski et al., 2011; Lai et al., 2006). Additionally, absorption of ultrasound energy gives rise to thermal effects which could alter the neuronal excitability or activate thermally sensitive ion channels (Constans et al., 2018). It is also very possible that several of these phenomena are activated in concert and synergistically cause activation.

The majority of studies exploring FUS neurostimulation and its optimal parameters have been carried out in humans or mammalian models (Fomenko et al., 2018). However, these nervous systems are quite complex at the network and molecular level. In order to gain a better understanding of how FUS stimulation affects neural activity, investigations at a cellular level or in a simple animal model would be beneficial. Recent publications report the use of invertebrate animals such as the common earthworm or the medicinal leech to study the effects of FUS (Collins and Mesce, 2020; Vion-Bailly et al., 2019). The FUS investigation with earthworms has a very straightforward methodology, but is limited by only being able to detect effects in the giant axons. We propose the California sea hare (*Aplysia californica*) as a new animal model for FUS stimulation research. Similar to the leech, *Aplysia californica* is a standard animal model for neurobiological study, having been used by researchers for over fifty years. The abdominal ganglion preparation is suitable for systematic evaluation of stimulation parameters; the ganglion consists of large, identifiable neurons whose diameters can exceed those of leech neurons by an order of magnitude, and whose axon pathways have been mapped, enabling convenient extracellular and intracellular recordings (Frazier et al., 1967). Further, the ganglion remains viable and electrically active for hours or even days when perfused with fresh, chilled artificial saline. Thus, this system provides an ideal environment for enabling extended experiments testing a range of stimulation parameters in a single sample.

In this work, we built a system for FUS stimulation of *ex-vivo Aplysia californica* abdominal ganglia that allows for stimulation at four distinct ultrasound frequencies: 0.515 MHz, 1.1 MHz, 1.61 MHz, 3.41 MHz. Using continuous wave FUS of varying pulse durations and pressure levels, we stimulated the ganglia at all four frequencies and present quantitative comparison of the stimulation outcomes. Further, we show that the responses to FUS are stable and comparable to responses elicited by electrical stimulation. Due to the ability to perform long experimentation on the order of hours, this system is suitable for systematic evaluation of optimal sonication parameters and studying the effects of varying ultrasound frequency.

2. Materials and methods

2.1. Focused ultrasound system

We designed the experimental setup to be compatible with two single-element FUS transducers, allowing us to stimulate the sample with four distinct frequencies. Transducer H-151 (Sonic Concepts, Bothell, WA) – diameter 64 mm, radius of curvature 100 mm – can be operated at a fundamental frequency of 1.1 MHz or a third harmonic frequency of 3.41 MHz. Transducer H-204 (Sonic Concepts, Bothell, WA) – diameter 87.19 mm, radius of curvature 63.2 mm – can be operated at a fundamental frequency of 0.515 MHz or a third harmonic frequency of 1.61 MHz. The sinusoidal ultrasound driving signal of an appropriate frequency was generated by a function generator (AFG1062, Tektronix, Beaverton, OR) and amplified with a 53-dB RF power amplifier (1020 L, E&I, Rochester, NY). The RF amplifier output was passed through an impedance matching network (Sonic Concepts, Bothell, WA) and connected to the transducer. To couple ultrasound energy to the sample, we utilized a custom molded polyacrylamide cone with ultrasound gel (Aquasonic, Clinton Township, MI) applied to the interfaces.

2.2. Ultrasound-coupling cone

To produce the polyacrylamide cone, we 3-D printed a two-piece mold (a distinct mold was required for each of the two transducers due to different focal depths and shapes of the transducers). The parts are available for download at https://fmilab.com/open. The first piece was 3-D modeled (SolidWorks, SolidWorks Corp., Waltham, MA) based on the transducer geometry to replicate the curved surface. The second piece was modeled based on the shape of the FUS beam from geometry data provided by the manufacturer (Sonic Concepts, Bothell, WA). The tips of the cones were truncated to allow positioning of the sample in the middle of the ultrasound focus. We 3-D printed (Mini, Lulzbot, N Fargo, ND) the molds using polylactic acid (PLA, ESun, Commerce, CA) and assembled the pieces to allow polyacrylamide casting. We used Parafilm (Bemis Company, Neenah, WI) to create a watertight seal between the two pieces.

Polyacrylamide solution was prepared by mixing 167 mL of degassed DI water (> 13 MOhm-cm resistivity), 84 mL of 30% acrylamide/bisacrylamide solution (J63279AP, Alfa Aesar, Haverhill, MA), and 2.5 mL of 10% ammonium persulfate solution (250 mg of ammonium persulfate dissolved in 2.5 mL of DI water). The polyacrylamide solution was then mixed with 313 μL of TEMED crosslinker (N,N,N,N′-Tetramethyl-ethylenediamine, 411019, Millipore Sigma, Burlington, MA), poured into the 3-D printed mold, and allowed to crosslink for about 20 min. The mold pieces were then separated to remove the polyacrylamide focusing cone. To prevent damage and drying of the gel, the cone was stored in a water bath when not in use.

2.3. Ganglion stimulation setup

The system was designed around a stationary sample and a FUS transducer that could be moved to precisely tune the position of the beam. The stationary parts were attached to optical posts mounted on an optical breadboard (Nexus, Thorlabs, Newton, NJ) with 1/4"− 20 mounting holes. The parts included a 3-D printed platform and a cooling stage. The cooling stage was comprised of a Peltier device (thermoelectric cooler) connected to a temperature controller (Cornerstone TC-10, Dagan) with a thermocouple, internally routed tubing for perfusion of chilled, fresh saline, and a 35 mm petri dish with a glass coverslip bottom (MatTek). Variations of the temperature in the petri dish were less than 0.1 °C during all FUS stimuli. A thin layer of Sylgard coated the inner bottom of the petri dish, which enabled pinning of the ganglion to the bottom.

Positioning of the FUS beam was achieved using an XY linear translation stage (XYT1, Thorlabs, Newton, NJ) mounted on the breadboard below the cooling stage. We designed and 3-D printed an H-151 transducer mount that we fastened to the XY stage with screws. Next, we 3-D printed an H-204 transducer mount that was designed to insert into the H-151 mount and act as an adapter (3-D printed parts are available at https://fmilab.com/open). The focal depth of the two

transducers differed, but the H-204 adapter acted to bridge this gap, so the focus was at the same height for both transducers. The final piece was the polyacrylamide cone which served to couple the ultrasound energy to the sample. We applied a thin layer of ultrasound gel between the transducer and the cone and between the tip of the cone and the bottom of the petri dish.

The two levels were designed and mounted in a way that the petri dish opening was positioned above the center of the FUS transducer. However, due to small variations in sample placement in the dish between experiments, it was critical to precisely align the FUS beam prior to stimulation. The alignment was achieved through the translation stage, which had 13 mm of travel along both axes and was actuated by a micrometer screw with 10 μm graduations. The complete setup with the H-151 transducer is depicted in Fig. 1A, while Fig. 1B shows the H-204 with the adapter.

2.4. Ultrasound field characterization

We performed hydrophone measurements to characterize the ultrasound field inside the petri dish. Namely, we were interested in the pressure distribution and peak focal pressure values. We used a 0.5-mm needle hydrophone (N0500, Precision Acoustics, Dorchester, United Kingdom) with a frequency band of 0.1–20 MHz, and a submersible hydrophone preamplifier (HP, Precision Acoustics, Dorchester, United Kingdom). The system was connected to a DC coupler and generated voltages were recorded with an oscilloscope (TBS1202B, Tektronix, Beaverton, OR).

Before the measurements, we allowed the needle hydrophone to soak for 1 h. Then, we filled the petri dish with highly degassed deionized water (<3 ppm dissolved oxygen, > 13 MOhm-cm resistivity) and positioned the hydrophone in the middle of the ultrasound focus using a 3-D printed mount connected to a motorized XY stage (2xLNR502 stage, BSC203 stepper motor controller, Thorlabs, Newton, NJ). We then proceeded to measure the peak pressure values at the four frequencies of interest (0.515 MHz, 1.1 MHz, 1.61 MHz, 3.41 MHz). We generated short ultrasound pulses (10–20 cycles) of the appropriate frequency at low amplitudes (1–9 mV_{rms}) to construct a calibration curve. Peak pressure values for sine waves of 50, 100, and 150 mV_{rms} were extrapolated from the calibration curve. To obtain the spatial profile of the ultrasound field, we kept the amplitude constant and measured the peak pressure in a cross-section of the ultrasound focus. The motorized XY stage was used to record 32 samples with step sizes of 0.3125 mm for the 1.1 MHz and 1.61 MHz frequencies, 0.625 mm for the 0.515 MHz frequency, and 0.15625 mm for the 3.41 MHz frequency.

2.5. Aplysia abdominal ganglion preparation

Juvenile *Aplysia californica* (~5 g) were obtained from the National Resource for *Aplysia* at the University of Miami's Rosenstiel School of Marine and Atmospheric Sciences. They were shipped overnight to New England College, where they were housed in artificial seawater at 15 °C. Animals were exposed to a 12-hour alternating light regimen (lights on at 6:00 am and off at 6:00 pm). They were fed either red algae (*Agardhiella subulata*) from the National Resource for *Aplysia* or dried green seaweed (i.e., nori) from the local grocery store. On days of experiments, individual *Aplysia* were brought to Dartmouth College.

Animals were anesthetized by injection of 10–20 mL of 1 M $MgCl_2$. Animals were pinned, ventral side up, to the bottom of a 14-cm diameter Sylgard-lined dish filled with artificial saline (420 mM NaCl, 50 mM $MgCl_2$, 10 mM KCl, 10 mM $CaCl_2$, 10 mM D-glucose, and 10 mM HEPES buffer; all chemicals from Sigma-Aldrich). A longitudinal incision was made in the foot and the digestive tract was moved aside to expose the abdominal ganglion. Nerves were cut as distal from the abdominal ganglion as feasible and the ganglion was pinned ventral side up in the 35-mm diameter Sylgard-lined petri dish in the ultrasound setup described previously (see Fig. 1).

In the ultrasound setup, the ganglion temperature was maintained at 12–15 °C and was perfused with high-divalent cation saline (285 mM NaCl, 125 mM $MgCl_2$, 10 mM KCl, 10 mM $CaCl_2$, 10 mM D-glucose, and 10 mM HEPES buffer; all chemicals from Sigma-Aldrich) at a rate of 0.5 mL/min (Sakurai et al., 2016). The use of high-divalent cation saline has been demonstrated to reduce synaptic activity (Liao and Walters, 2002). This made it easier to observe the direct impacts of FUS stimulation on neurons.

2.6. Electrophysiology

Extracellular suction electrode recordings were obtained by drawing the right abdominal-pleural connective and the siphon nerve each into a glass electrode filled with high-divalent cation saline (Fig. 2). An extracellular amplifier (model 1800, A-M Systems, Sequim, WA) was used to acquire and amplify extracellular recordings from nerves. These signals were digitized with a PowerLab 4/35 (AD Instruments, Dunedin, New Zealand) at a sampling rate of 1 kHz. Data were recorded using LabChart (v7.3.8, AD Instruments, Dunedin, New Zealand). When comparing FUS to electrical stimuli, nerve stimulation was produced with LabChart and applied via the A-M Systems extracellular amplifier. The siphon nerve was used for nerve stimulation, which consisted of 5–10 V, 1 ms pulses at 20 Hz for 0.25–1 s. Electrophysiological data were exported to Matlab (R2018b, MathWorks, Natick, MA) for analysis.

2.7. Ultrasound stimulation and recording setup

A diagram depicting the experimental stimulation and recording hardware is shown in Fig. 3. The FUS transducer was driven by a sinusoidal wave of an appropriate frequency (0.515 MHz, 1.1 MHz,

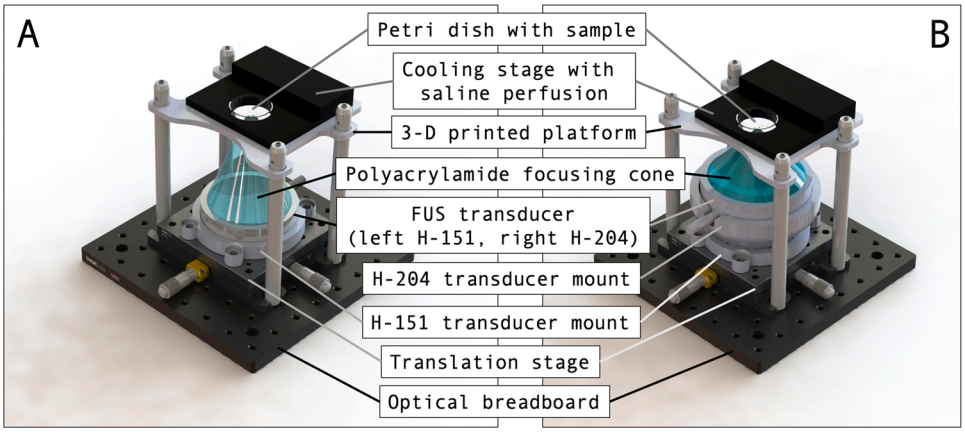

Fig. 1. (A) Ultrasound neurostimulation setup featuring an H-151 focused ultrasound transducer (fundamental frequency of 1.1 MHz, third harmonic frequency of 3.41 MHz). The sample is positioned in a petri dish mounted on a cooling stage, perfused with chilled artificial saline. Ultrasound energy is coupled to the sample through a custom molded polyacrylamide cone. The ultrasound beam can be precisely aligned with the sample using a 2-axis translation stage. (B) The setup shown with an H-204 transducer (fundamental frequency of 0.515 MHz, third harmonic frequency of 1.61 MHz). Switching between transducers involves inserting an adapter into the H-151 mount (ensuring that the ultrasound focus remains at the same height) and using a shorter coupling cone specific to the H-204 transducer.

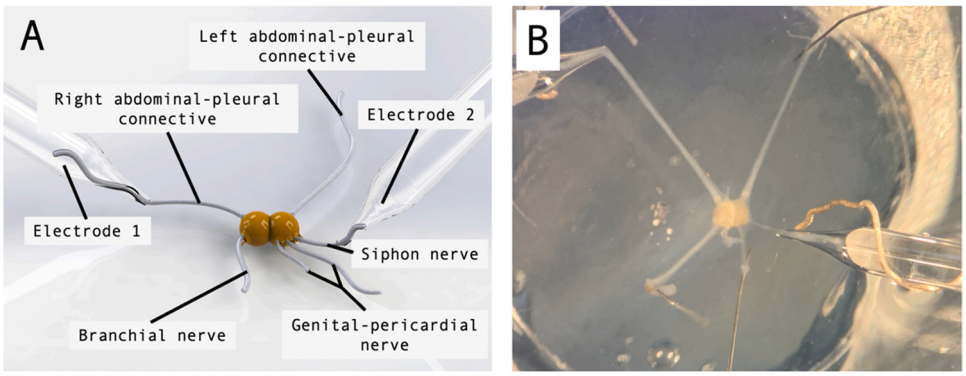

Fig. 2. (A) This schematic depicts the Aplysia abdominal ganglion, ventral side up and anterior towards the top of the image, with extracellular suction electrodes. In our experiments, we recorded electrophysiological signals from the right abdominal-pleural connective and the siphon nerve. (B) Photograph of the ganglion during experimentation.

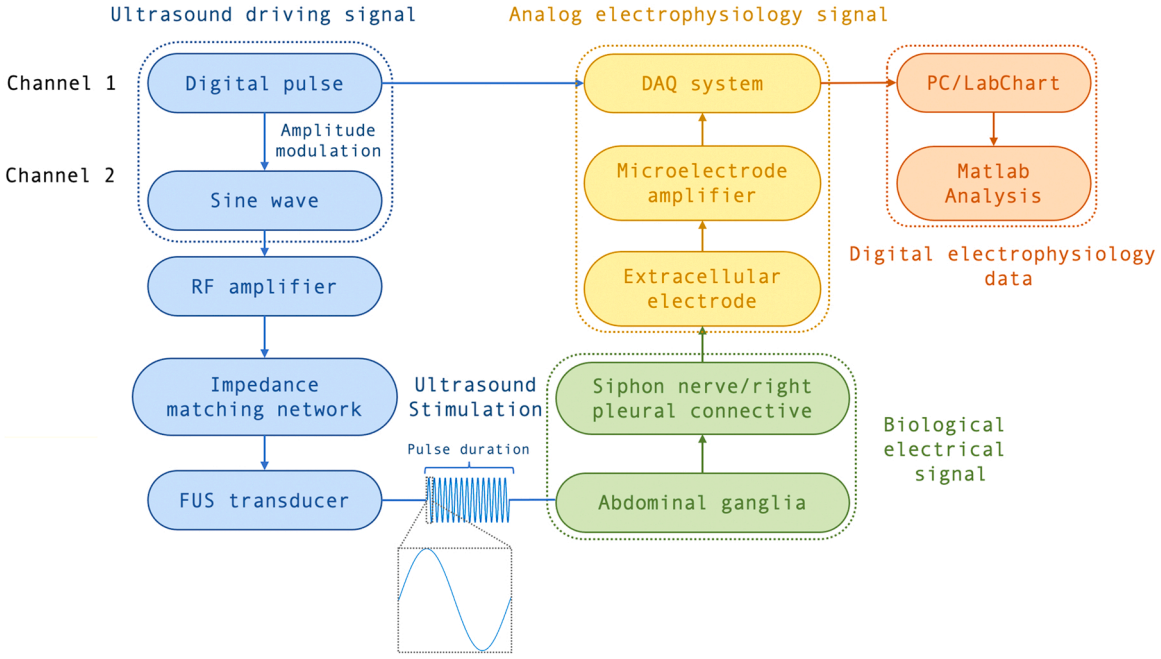

Fig. 3. Diagram depicting the generation of the ultrasound driving signal, electrophysiological recording of activity elicited by stimulation, and sampling of the signals.

1.61 MHz, or 3.41 MHz) created by the function generator. The amplitude of this sinusoidal wave was modulated by a digital pulse that controlled the stimulus timing and duration. The pulse wave channel was recorded by the PowerLab 4/35 data acquisition system (sampled at 2 kHz) to synchronize the stimulation with the electrophysiological recordings. The ultrasound-driving sine wave was amplified by an RF amplifier, providing a 53-dB gain. The amplified signal then passed through an impedance matching network into the FUS transducer. Ultrasound energy (coupled to the ganglion by our polyacrylamide cone) stimulated the sample, and the elicited electrical activity (voltage) was recorded from the two nerves (right abdominal-pleural connective and siphon nerve) using extracellular electrodes. Data analysis was performed in Matlab.

2.8. Stimulation of the abdominal ganglion and evaluation of FUS parameters

We tested FUS stimulation at four distinct carrier frequencies: 0.515 MHz, 1.1 MHz, 1.61 MHz, and 3.41 MHz. For each frequency, we varied the stimulus duration (1 ms, 10 ms, 100 ms, 1 s) at three different voltage levels of the driving sine wave (50 mV_{rms}, 100 mV_{rms}, 150 mV_{rms}). The relationship between sine wave voltage, ultrasound peak focal pressure (as measured by a hydrophone) and calculated spatial peak pulse average intensity (I_{SPPA}) is shown in Table 1. The experiment began with a 1 ms/50 mV stimulus applied to the ganglion, followed by an increase in voltage to 100 mV and 150 mV. This paradigm was repeated for 10 ms and 100 ms pulse durations. At the 1 s pulse duration, we only tested 50 and 100 mV amplitudes due to concerns about possible tissue damage at 150 mV. Each combination of stimulus duration/amplitude was applied twice, and we allowed 5 min to pass between stimulations to allow the ganglion electrical activity to return to its baseline. Four animals were used to test each frequency.

The experiment yielded a set of 16 electrophysiological recordings (4 animals x 2 nerves x 2 stimulation events) for each of the 11 parameters (stimulus duration/amplitude combination) at each of the four frequencies. The recordings were processed in Matlab and organized into vectors containing 30 s of data prior to a stimulation and 30 s of data post-stimulation. Automated noise floor detection was used to threshold the data and count individual spikes. The ratio of the number of spikes in the post-stimulus vector to the number of spikes in the pre-stimulus

Table 1
Ultrasound peak focal pressure values and spatial peak pulse average intensities (I_{SPPA}) for the four tested frequencies (0.515 MHz, 1.1 MHz, 1.61 MHz, 3.41 MHz) at the driving sine wave amplitudes that we utilized in the stimulation experiments.

	0.515 MHz		1.1 MHz		1.61 MHz		3.41 MHz	
	Peak Focal pressure (MPa)	I_{SPPA} (W/cm^2)	Peak Focal pressure (MPa)	I_{SPPA} (W/cm^2)	Peak Focal pressure (MPa)	I_{SPPA} (W/cm^2)	Peak Focal pressure (MPa)	I_{SPPA} (W/cm^2)
50 mV	1.11	41.1	2.61	227	0.258	2.22	0.506	8.52
100 mV	2.22	165	5.22	909	0.515	8.85	1.01	34.1
150 mV	3.33	371	7.83	2050	0.773	20.0	1.52	76.7

vector was calculated. This fold-change in post-stimulus spiking was used as a quantitative measure of the response induced by FUS stimulation. The data from right abdominal-pleural connective and siphon nerve were analyzed separately since different levels of baseline spiking and excitability were observed in these nerves. To assess the statistical significance of recorded responses, the pre-stimulus and post-stimulus vectors were split into two 15 second halves. A control (no-stimulus) population was obtained by dividing the number of spikes in the last 15 s of the pre-stimulus vector by the number of spikes in the first 15 s of the pre-stimulus vector. The population corresponding to the FUS stimulus was obtained by dividing the number of spikes in the first 15 s of the post-stimulus vector by the number of spikes in the first 15 s of the pre-stimulus vector. These two populations were then compared using a paired, two-sided Wilcoxon signed rank test.

2.9. Evaluating the repeatability of ultrasound stimulation

After testing a range of stimulation parameters, the next set of experiments was to determine if FUS stimulation could be repeated without a decrease in the elicited response. As a comparison, we used electrical stimulation of the siphon nerve administered through the extracellular electrode. The experiments were performed with the H-151 transducer at 1.1 MHz frequency, which elicited robust and consistent electrical responses in the prior experiments. At the beginning of each experiment, we identified the animal specific FUS stimulation parameters that reliably caused significant activation (typically 1 s pulse duration, 70–80 mV_{rms} sine wave amplitude). Similarly, we identified an electrical stimulus yielding a similar electrophysiological response (1 ms pulses at 20 Hz, 0.25–1 s duration, voltage 5–10 V). The aim was to compare the responses of three consecutive FUS or electrical stimulation events carried out with different time intervals (1 min, 5 min, or 10 min).

First, we applied three FUS stimuli every 1 min, followed by three electrical stimuli every 1 min. After a 10-minute rest period, we applied FUS and electrical stimuli in 5-minute intervals. After another 10-minute rest, we carried out the stimulations in 10-minute intervals. The experiment was repeated on 9 animals.

The recordings were processed in Matlab in the same fashion as described in Section 2.8, yielding spiking fold-change values. For each time interval, we normalized all FUS responses to the median of the first FUS response and all electrical responses to the median of the first electrical response. This way, we obtained the relative comparison between the first, second, and third responses for FUS or electrical stimulation at each of the three intervals. To determine whether there were any statistically significant changes in the responses among these three consecutive stimulations, we utilized a paired, two-sided Wilcoxon signed rank test. The right-abdominal pleural connective and siphon nerve data were analyzed separately.

3. Results

We carried out hydrophone measurements of the ultrasound peak focal pressure for the four frequencies of interest as reported in Table 1. The lowest peak pressures were measured at the 1.61 MHz frequency (50 mV sine wave translated to 0.258 MPa), followed by 3.41 MHz (0.506 MPa at 50 mV), 0.515 MHz (1.11 MPa at 50 mV), and 1.1 MHz (2.61 MPa at 50 mV). Next, we investigated the spatial characteristics of the ultrasound field in the petri dish. We generated stimuli with a constant amplitude and, using the hydrophone mounted on a motorized stage, we scanned a cross-section of the focus, taking 32 peak pressure measurements at all four frequencies. The shape of the focus for each frequency as well as the focal width (determined by the full width at half maximum – FWHM) are shown in Fig. 4. The narrowest focus was found at the 3.41 MHz frequency (1.05 mm), followed by 1.1 MHz (3.34 mm), 0.515 MHz (4.71 mm), and 1.61 MHz (7.90 mm). The ultrasound focus had circular symmetry for all 4 tested frequencies. We scanned cross-sections of the focus perpendicular to the ones reported in Fig. 4 and obtained similar profiles.

Next, we applied continuous wave FUS stimulation at the four frequencies of interest to the *ex-vivo Aplysia* abdominal ganglion. We varied stimulus intensities and pulse durations to produce a range of electrical responses in the right abdominal-pleural connective and the siphon

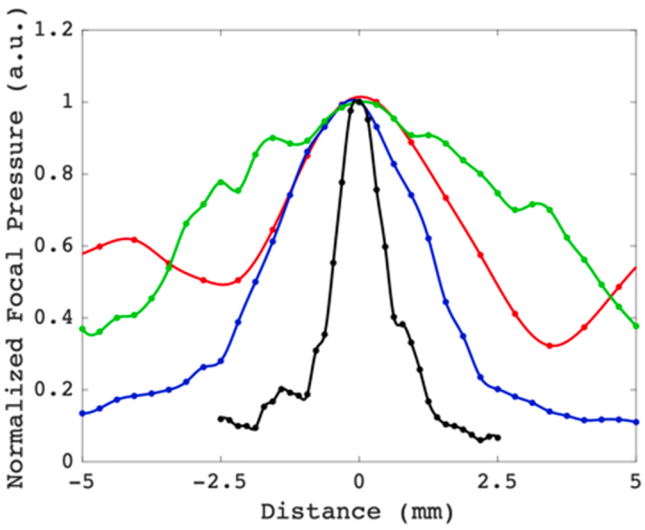

	Focal size (FHWM)
0.515 MHz	4.71 mm
1.1 MHz	3.34 mm
1.61 MHz	7.90 mm
3.41 MHz	1.05 mm

Fig. 4. Normalized peak pressure values measured in a cross-section of the ultrasound focus in the petri dish, illustrating the shape of the focus and the focal width. The bottom portion of the figure reports the full-width half maximum (FWHM) as the focal size for each frequency.

nerve. For each frequency, we tested stimulation durations of 1 ms, 10 ms, 100 ms, and 1 s. To vary FUS intensity, we utilized driving sine wave amplitudes of 50 mV_{RMS}, 100 mV_{RMS}, and 150 mV_{RMS} (the relationship between voltage and peak focal pressure is shown in Table 1). The stimulus was focused in the center of the ganglion and the elicited activation was recorded extracellularly from the two nerves. The results are qualitatively represented in raster plots and average spiking frequency plots in Fig. 5. Enhanced spike density in the raster plot and increased average spiking frequency indicates a successful activation of the ganglion induced by the FUS stimulus.

To quantitatively compare the responses to different stimulation parameters, we calculated an average post-stimulus fold-change in spiking as the ratio of the number of spikes in the 30 s following the stimulus to the number of spikes in the 30 s prior to the stimulus. The fold-change values are represented in heat maps in Fig. 6. A value of 1 represents no change in spiking following the stimulus, a value greater than 1 signifies a spiking increase, and a value lower than 1 means that the spiking frequency decreased.

The siphon nerve was about six times more active than the right abdominal-pleural connective at baseline (the 30 s pre-stimulus period averaged 21.8 spikes for the right abdominal-pleural connective, compared to 121 spikes for the siphon nerve). Additionally, we found that the siphon nerve was nearly twice as excitable as the abdominal-pleural connective. Across all stimulation parameters and all frequencies, FUS yielded an average 6.94-fold increase in the siphon nerve spiking, while only a 3.68-fold increase was observed in the right abdominal-pleural connective. Hence, we report the results for all experiments for both nerves separately.

At all four tested frequencies, the overall trend was that the response to FUS stimulation increased with both stimulus duration and peak pressure. The 3.41-MHz stimulation parameters were the least efficient in eliciting a response (Fig. 6D). The calculated fold-change values indicated little to no spiking increase with a maximum fold-change of 3.2 in the right-abdominal pleural connective (1.52 MPa/1 ms) and 8.7 in the siphon nerve (1.52 MPa/100 ms). Further, all recorded spiking increase responses were determined to be not statistically significant.

Improved results were achieved with the 1.61 MHz stimulation parameters (Fig. 6C). Statistically significant spiking increase responses were observed in 2/11 parameters in the right abdominal-pleural connective with a maximum fold-change of 5.3 (0.515 MPa/1 s). In the siphon nerve, 3/11 parameters produced statistically significant responses with a maximum fold-change of 19.4 (0.515 MPa/100 ms).

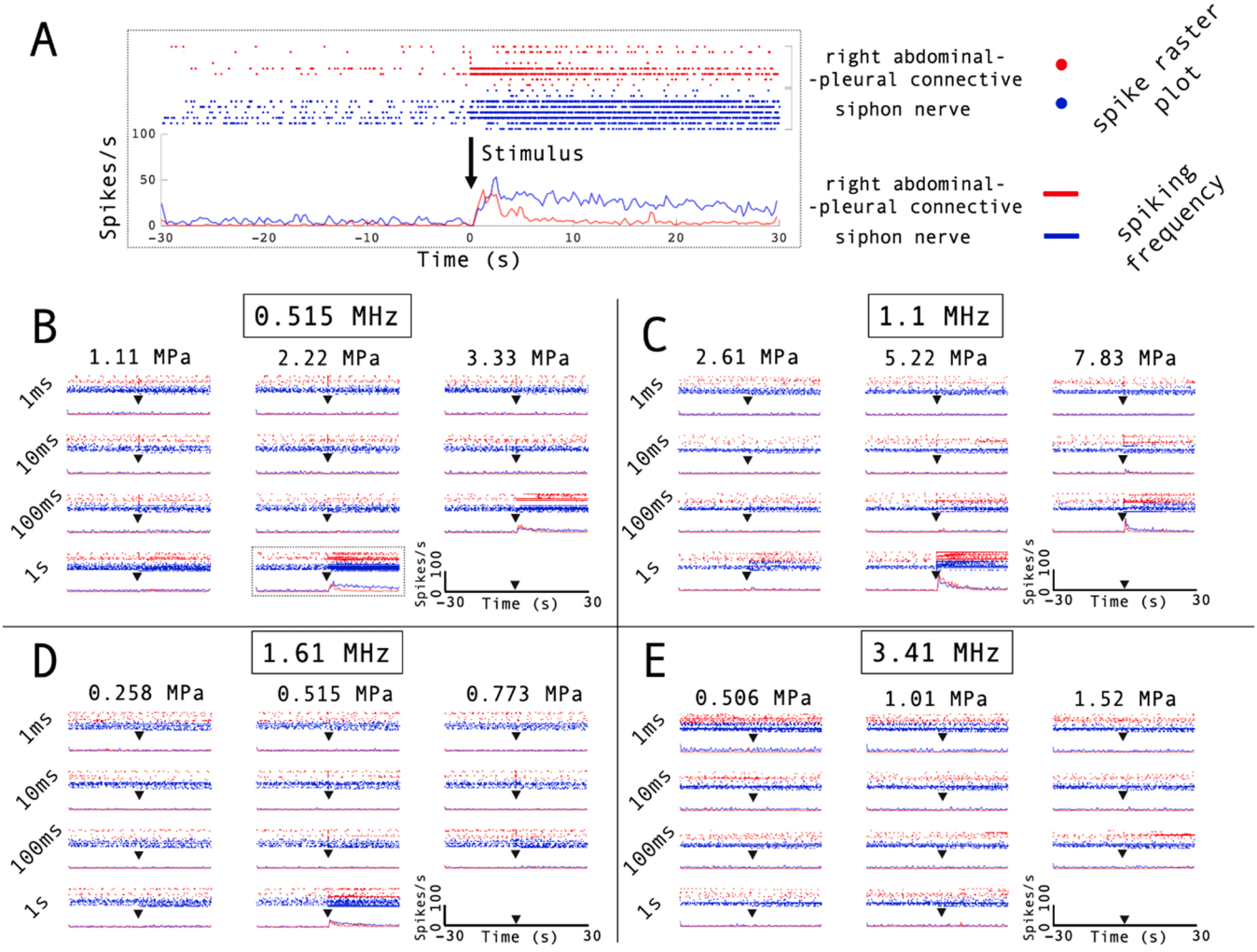

Fig. 5. (A) An enlarged plot of the responses to one set of the stimulation parameters (0.515 MHz frequency, 1-s pulse duration, 2.22-MPa peak pressure). The top portion of the plot represents a spike raster plot with eight right abdominal-pleural connective recordings shown in red and eight siphon nerve recordings shown in blue. Each dot represents a single spike. The raster plot is on the same time scale as the average spiking frequency plot in the bottom portion, showing spikes and spiking frequencies for 30 s before and after the ultrasound stimulus. The spiking frequency plot shows two traces: the red trace represents the average spiking frequency calculated from the abdominal-pleural connective recordings, while the blue trace represents the average spiking frequency for the siphon nerve. (B) The responses for all sets of stimulation parameters are shown for the 0.515 MHz ultrasound frequency. Each row represents one pulse duration value, and each column shows one peak pressure setting. The same plots are shown for the 1.1-MHz (C), 1.61-MHz (D), and 3.41-MHz (E) ultrasound frequencies.

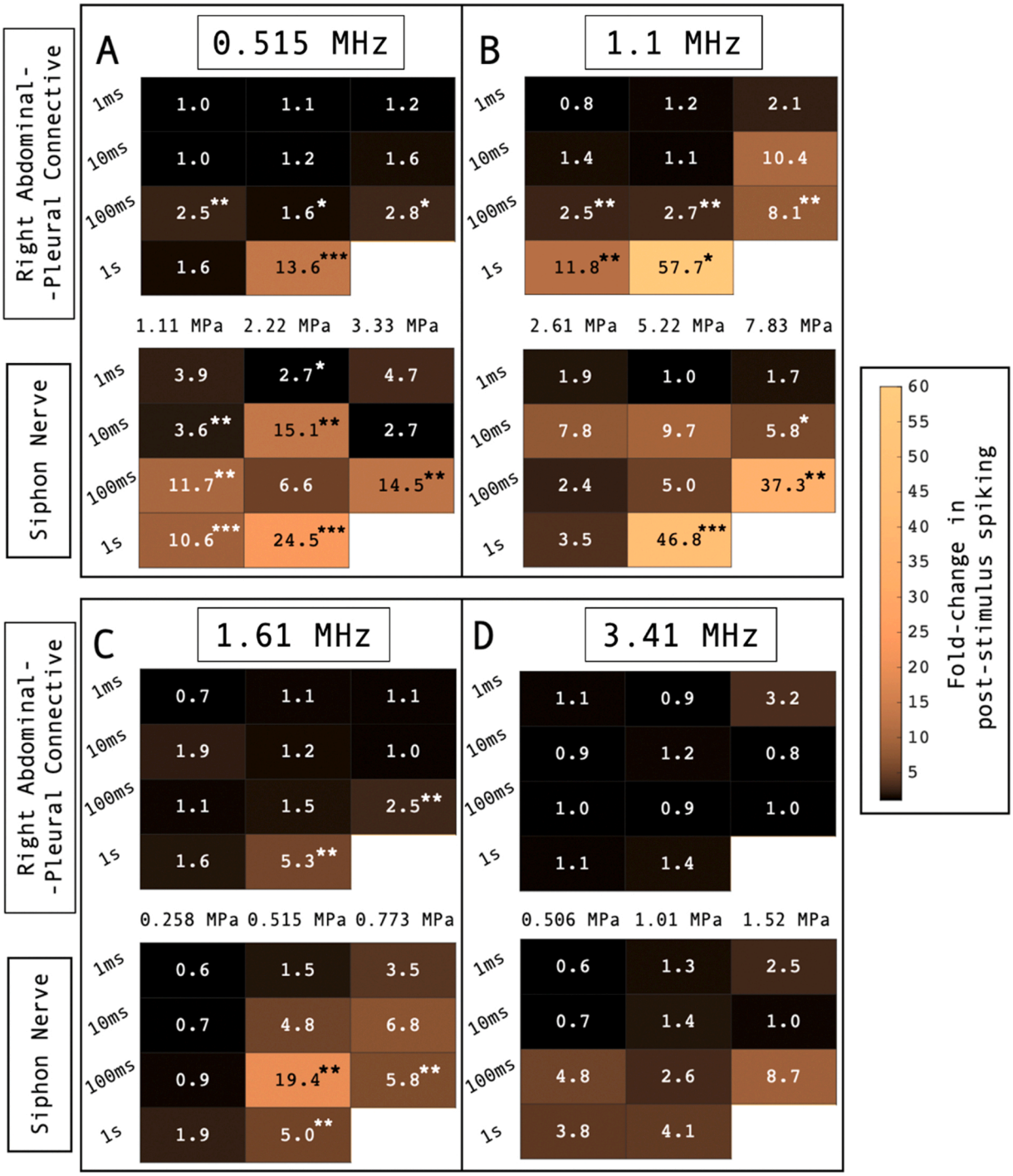

Fig. 6. Quantitative comparison of the levels of activation elicited by different stimulation parameters. (A) The top heatmap shows responses recorded from the right abdominal-pleural connective and the bottom map is from the siphon nerve at 0.515 MHz stimulation. Each row corresponds to one stimulus duration and each column one peak focal pressure setting. The values in the heatmap represent the fold-change in spiking following the stimulus (* $p < 0.05$, ** $p < 0.01$, *** $p < 0.001$). The remaining heatmaps show responses for 1.1 MHz stimulation (B), 1.61 MHz stimulation (C), and 3.41 MHz stimulation (D).

Our 1.1 MHz stimuli led to efficient activation of the abdominal ganglion with robust responses observed using most stimulation parameters (Fig. 6B). In the right abdominal-pleural connective, spiking increase responses to 5/11 parameters were statistically significant and the maximum fold-change value was 57.7 (5.22 MPa/1 s). For the siphon nerve, 3/11 parameters produced statistically significant responses with a maximum fold-change of 46.8 (5.22 MPa/1 s).

Similarly, we saw efficient neural activation using FUS parameters with the lowest frequency of 0.515 MHz (Fig. 6A). In 4/11 parameters in the right abdominal-pleural connective, the spiking increase responses were statistically significant, and the maximum fold-change value was 13.6 (2.22 MPa/1 s). In the siphon nerve, statistically significant responses were found in 7/11 stimulation parameters with a maximum fold-change of 24.5 (2.22 MPa/1 s).

Next, we investigated if the FUS-induced abdominal ganglion activation was repeatable and consistent and if the interval between individual stimulation events influenced neural responses. Additionally, we included electrical stimulation in this experiment to determine if FUS

stimulation responses differed in stability and consistency from responses elicited by electrical stimulation. We tested three consecutive FUS and electrical stimulation events with 1-minute, 5-minute, and 10-minute intervals. For all time intervals and both stimulation modalities, we normalized the three consecutive responses to the median of the first response to gain relative comparison. The results are shown in Fig. 7.

Due to the previously observed differences in baseline activity and excitability in the abdominal-pleural connective and siphon nerves (Figs. 5 and 6), we again report the results for both nerves separately. The results demonstrate that we were able to repeatedly activate the ganglion with three consecutive FUS and electrical stimuli. The responses were generally stable, and we found no evident differences between repeated FUS and electrical stimulation. In isolated cases, statistical analysis showed a significant increase or decrease in the response strength. However, due to the lack of a consistent trend in response strength, we attribute these differences to the modest population of ganglia used for comparison. Indeed, when the 12 trials for each animal were analyzed together, a one-way ANOVA test showed no significant differences ($p = 0.22$), indicating that prior stimuli do not affect future excitability at these stimulation parameters. Overall, the method was found robust and suitable for repeated FUS stimulation of the *Aplysia* abdominal ganglion.

4. Discussion

Our FUS stimulation system utilizes a custom molded polyacrylamide cone to couple ultrasound energy to a sample inside a saline-filled glass bottom petri dish. This design minimizes the number of components that need to be submerged for acoustic coupling and reduces the amount of required liquid, which simplifies temperature control of the sample. However, there are two key differences in the ultrasound field that the sample experiences. First, the ultrasound beam has to pass through multiple different media en route to the sample. There is a thin layer of ultrasound gel between the transducer and the cone, then several cm of polyacrylamide, another layer of ultrasound gel, a thin layer of glass, and, finally, a layer of Sylgard which facilitates pinning of the ganglion to the bottom of the petri dish. Thus, some of the ultrasound energy is attenuated before the beam reaches the focus. Second, the ultrasound focus is only a few mm away from the water/air boundary. This leads to reflections of the ultrasound energy and formation of standing waves.

Due to these differences, the peak focal pressure and the shape of the focus in the petri dish deviate from data provided by the manufacturer. To obtain reliable information about the ultrasound field in the petri dish and to compare the transducers, we utilized a needle hydrophone to measure the peak pressure values and focal widths for the four frequencies of interest. We found that the third harmonic frequencies (1.61 MHz and 3.41 MHz) produced lower peak pressures than the fundamental frequencies for both transducers. Further, the H-204 transducer produced lower pressures then the H-151 transducer at the same driving sine wave voltages at both the fundamental and the third harmonic frequencies. As for the shape of the focus, it was found to have circular symmetry at all four frequencies, as expected. The focal widths for all four frequencies were larger than the theoretical values provided by the manufacturer. These findings highlight the importance of evaluating the ultrasound field when designing a system for neurostimulation, especially when ultrasound reflections and standing wave formations may be involved.

There have been numerous studies investigating the optimal ultrasound parameters for neurostimulation (Kim et al., 2014; King et al., 2013; Tufail et al., 2011; S. Wang et al., 2020; X. Wang et al., 2020; Yoon et al., 2019). Most consider the effects of changing ultrasound intensity, stimulation duration, and duty cycle or pulse repetition frequency in the case of pulsed ultrasound. Ultrasound carrier frequency is another important variable as it directly affects the heating effects, acoustic cavitation, acoustic radiation force, or absorption rate. However, studies investigating neurostimulation effects of changing ultrasound frequency are less common (Ye et al., 2016). Our goal was to design a system that would allow for studying multiple ultrasound frequencies. Using a two-transducer design, we built a FUS stimulation system for neurostimulation at frequencies of 0.515 MHz, 1.1 MHz, 1.61 MHz, and 3.41 MHz. Combined with the advantages of the *Aplysia* abdominal ganglion (such as the feasibility of very long recordings), our system is well suited for a systematic evaluation of ultrasound parameters to determine optimal stimulation settings.

To demonstrate the capability of our system, we applied multi-frequency stimulation to *ex-vivo Aplysia* abdominal ganglia and observed varying levels of activation. The spectrum of responses ranged from a subtle activation to a nearly 60-fold increase in spiking. The siphon nerve was in most cases more active and more excitable, and we found it better suited for studying the effects of FUS stimulation. This may have been due to the presence of a larger number of axons in the siphon nerve, compared to the pleural connective (Coggeshall, 1967), and the fact that a number of identified neurons that project out the connective (e.g., neurons R1 and R2) tend to be relatively large and silent (Frazier et al., 1967). These nerves/connectives were selected for these experiments due to the relative ease with which they could be cut distal to the ganglion and provide a long enough segment for insertion in a suction electrode.

While a large-scale systematic study investigating the effects of changing ultrasound frequency was not the objective of this work, some preliminary comparisons between frequencies can be drawn from our results. The 3.41 MHz third harmonic frequency was the least effective and failed to produce statistically significant increase in the post-stimulus spiking (even at the highest FUS pressure of 1.52 MPa and longest pulse duration of 1 s). For a comparison with the other third harmonic frequency, 0.515 MPa stimulation at 1.61 MHz produced average spiking fold-changes as high as 19.4 while 0.506 MPa stimulation at 3.41 MHz led to no statistically significant increase in spiking. As for the fundamental frequency comparison, 2.22 MPa stimulation at 0.515 MHz appeared more effective than 2.61 MPa stimulation at 1.1 MHz – in the siphon nerve the maximum average fold change was 24.5 for 0.515 MHz and only 7.8 for 1.1 MHz; in the abdominal-pleural connective the highest average fold-change was 13.6 at 0.515 MHz compared to 11.8 at 1.1 MHz. These comparisons are consistent with a hypothesis that lower frequency FUS activates the *Aplysia* abdominal ganglion more efficiently and higher pressures are required with increasing frequency. However, an in-depth study with matching peak focal pressure values across frequencies is needed to provide further evidence.

Recent ultrasound neurostimulation studies in invertebrates report a loss of sensitivity to ultrasound during repeated stimulation which can be reversed by waiting a significant amount of time (Vion-Bailly et al., 2019). In isolated cases, only a single response was elicited with no further successful activations (Wright et al., 2015). We aimed to evaluate whether FUS stimulation of the *Aplysia* abdominal ganglion was repeatable and if the responses were stable. We investigated the elicited responses to three consecutive FUS stimuli applied every 1 min, 5 min, and 10 min. Further, we applied three consecutive electrical stimuli with the same time intervals for stability comparison. We were able to elicit three consecutive responses to both FUS and electrical stimulation in both nerves for all tested time intervals. The responses were generally stable, and we found no differences in responses elicited by FUS and electrical stimulation. In a few isolated cases, statistical analysis revealed a statistically significant increase or decrease in some consecutive responses. However, we hypothesize that this was due to the small sample size and high variation in the recorded responses (particularly in the 1-minute interval where the amount of time between stimuli was not sufficient to allow the electrical activity to return to its baseline). Overall, successful neural activation was achieved in all cases, suggesting that FUS is suitable for repeated stimulation of the *ex-vivo Aplysia* abdominal ganglion.

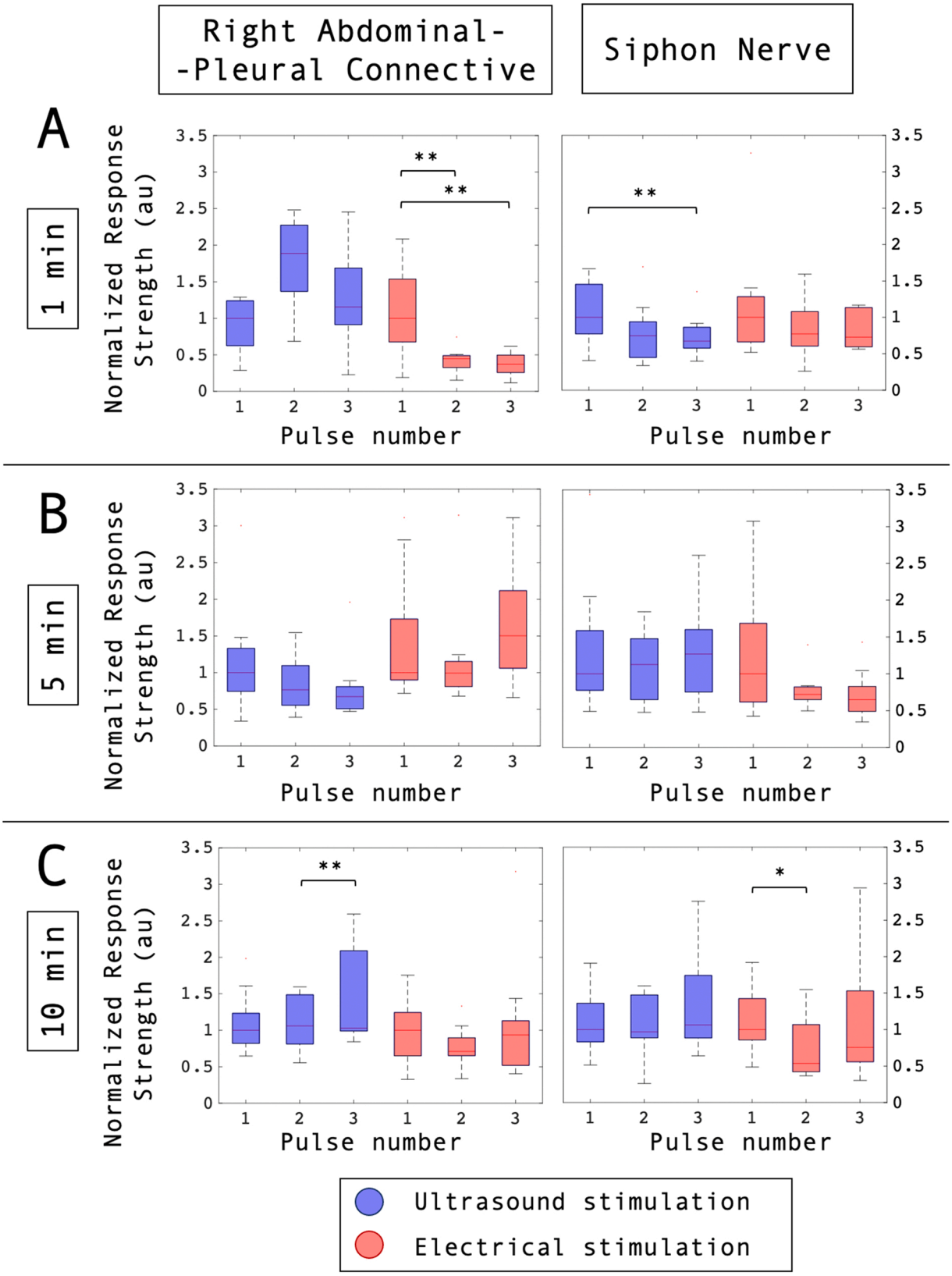

Fig. 7. Evaluation of the stability and consistency of responses to ultrasound and electrical stimulation in different time intervals. (A) Responses to three consecutive ultrasound stimuli (blue) and electrical stimuli (red) applied every 1 min. The ultrasound responses are normalized to the median of the first ultrasound response and the electrical responses are normalized to the median of the first electrical response. The left boxplot represents data for the right abdominal-pleural connective, and the right boxplot represents data for the siphon nerve. The remaining panels show comparisons of responses for stimulation events applied in 5-min intervals (B) and 10-min intervals (C). *$p < 0.05$; **$p < 0.01$.(For interpretation of the references to color in this figure legend, the reader is referred to the web version of this article).

The majority of studies investigating the neural effects of FUS and optimization of stimulation parameters are carried out in humans and other mammalian systems (Fomenko et al., 2018; Wang et al., 2020). However, there are a number of advantages to using an invertebrate nervous system to assess variation in FUS stimulations and the mechanism underlying these effects. First, the neural preparation is more robust, enabling longer experiments. For example, ganglia isolated from *Aplysia* will function for many hours, and even days, if kept slightly chilled (~12–15 °C) and perfused at a low rate (~0.5 mL/min) with artificial saline. Second, available time for an experiment is increased by the fact that the preparation of the isolated nervous tissue is very quick – less than an hour from an intact animal to extracellular recordings ready for FUS stimulation. Last, the *ex-vivo* ganglion preparation constitutes a largely intact neural structure with all of the neurons present, including their synaptic connections in the neuropil of the ganglion. This contrasts with the more limited cell connectivity of mammalian brain slices or the artificial and significantly altered landscape of neurons in culture. Thus, future studies of network-level responses could be pursued.

Ultrasound experiments have been done recently with other invertebrate nervous systems, including the crayfish *Procambarus clarkii* (Lin et al., 2019), the earthworm *Lumbricus terrestris* (Vion-Bailly et al., 2019), and the medicinal leech *Hirudo verbana* (Collins et al., 2021; Collins and Mesce, 2020). Of note, Collins and Mesce (2020) provided evidence for ultrasound-induced artifacts with intracellular recording, suggesting that other methodologies, such as the extracellular recordings that we used in our study, may be preferable methods for accurately assessing neural effects of ultrasound stimulation. Our FUS system with the *Aplysia* abdominal ganglion adds to these recent experiments, and does so with arguably one of the most studied invertebrate nervous systems, aside from *Caenorhabditis elegans* and *Drosophila melanogaster*. Together, these invertebrate preparations provide excellent promise for future investigations on both optimal parameters for FUS stimulation and the mechanism(s) underlying neural responses to ultrasound.

5. Conclusions

We built a system for FUS stimulation of *ex-vivo Aplysia californica* abdominal ganglia. The system utilizes 3-D printed parts, a custom molded ultrasound coupling cone, an XY translation stage for a precise alignment of the ultrasound beam, a cooling stage with perfusion of chilled artificial saline, extracellular electrodes for electrophysiology recordings and electrical stimulation, and one of two single element transducers allowing for stimulation at four distinct frequencies (0.515 MHz, 1.1 MHz, 1.61 MHz, 3.41 MHz). To test the system, we stimulated *ex-vivo Aplysia* abdominal ganglia using a range of stimulation parameters and observed a wide spectrum of elicited responses. Further, we tested how repeatable ultrasound stimulation is and found no apparent differences in consistency when compared to electrical stimulation making more use of this stimulation in other preparations. Due to the multi-frequency capability and the ability of the *Aplysia* abdominal ganglion preparation to remain electrically active for hours or even days, our setup is ideal for an in-depth study of the effects of frequency selection on ultrasound neurostimulation in invertebrate systems. Since ultrasound frequency affects heating, acoustic cavitation, and other ultrasound bioeffects, a detailed study in an animal model that is simpler and more robust than the mammalian brain could provide new insight into the mechanisms of action behind ultrasound neurostimulation.

CRediT authorship contribution statement

Tomas Jordan: Conceptualization, Methodology, Investigation, Data curation, Writing – original draft, Visualization. **James M. Newcomb:** Conceptualization, Methodology, Investigation, Writing – review & editing, Funding acquisition. **Michael B. Hoppa:** Conceptualization, Methodology, Writing – review & editing, Funding acquisition. **Geoffrey P. Luke:** Conceptualization, Methodology, Writing – review & editing, Project administration, Funding acquisition.

Acknowledgements

This work was supported by NIH grants R21EY029422, 3P20GM103506-10S1, and R03NS118125.

Conflicts of Interest

The authors declare no conflicts of interest.

References

Bachtold, M.R., Rinaldi, P.C., Jones, J.P., Reines, F., Price, L.R., 1998. Focused ultrasound modifications of neural circuit activity in a mammalian brain. Ultrasound Med. Biol. 24, 557–565. https://doi.org/10.1016/S0301-5629(98)00014-3.

Blackmore, J., Shrivastava, S., Sallet, J., Butler, C.R., Cleveland, R.O., 2019. Ultrasound neuromodulation: a review of results, mechanisms and safety. Ultrasound Med. Biol. 45, 1509–1536. https://doi.org/10.1016/j.ultrasmedbio.2018.12.015.

Brohawn, S.G., 2015. How ion channels sense mechanical force: insights from mechanosensitive K2P channels TRAAK, TREK1, and TREK2: mechanical gating of K2P channels. Ann. N. Y. Acad. Sci. 1352, 20–32. https://doi.org/10.1111/nyas.12874.

Chivers, R.C., Hill, C.R., 1975. Ultrasonic attenuation in human tissue. Ultrasound Med. Biol. 2, 25–29. https://doi.org/10.1016/0301-5629(75)90038-1.

Choi, J.B., Lim, S.H., Cho, K.W., Kim, D.H., Jang, D.P., Kim, I.Y., 2013. The effect of focused ultrasonic stimulation on the activity of hippocampal neurons in multi-channel electrode, in: 2013 6th International IEEE/EMBS Conference on Neural Engineering (NER). Presented at the 2013 6th International IEEE/EMBS Conference on Neural Engineering (NER), IEEE, San Diego, CA, USA, pp. 731–734. https://doi.org/10.1109/NER.2013.6696038.

Coggeshall, R.E., 1967. A light and electron microscope study of the abdominal ganglion of Aplysia californica. J. Neurophysiol. 30 (6), 1263–1287. https://doi.org/10.1152/jn.1967.30.6.1263.

Collins, M.N., Legon, W., Mesce, K.A., 2021. The inhibitory thermal effects of focused ultrasound on an identified, single motoneuron. eNeuro 8 (2), ENEURO.0514-20.2021. https://doi.org/10.1523/ENEURO.0514-20.2021.

Collins, M.N., Mesce, K.A., 2020. Focused ultrasound neuromodulation and the confounds of intracellular electrophysiological investigation. ENeuro 7. https://doi.org/10.1523/ENEURO.0213-20.2020. ENEURO.0213-20.2020.

Constans, C., Mateo, P., Tanter, M., Aubry, J.-F., 2018. Potential impact of thermal effects during ultrasonic neurostimulation: retrospective numerical estimation of temperature elevation in seven rodent setups. Phys. Med. Biol. 63, 025003 https://doi.org/10.1088/1361-6560/aaa15c.

Fomenko, A., Neudorfer, C., Dallapiazza, R.F., Kalia, S.K., Lozano, A.M., 2018. Low-intensity ultrasound neuromodulation: an overview of mechanisms and emerging human applications. Brain Stimul. 11, 1209–1217. https://doi.org/10.1016/j.brs.2018.08.013.

Frazier, W.T., Kandel, E.R., Kupfermann, I., Waziri, R., Coggeshall, R.E., 1967. Morphological and functional properties of identified neurons in the abdominal ganglion of *Aplysia californica*. J. Neurophysiol. 30, 1288–1351. https://doi.org/10.1152/jn.1967.30.6.1288.

Fry, F.J., Ades, H.W., Fry, W.J., 1958. Production of reversible changes in the central nervous system by ultrasound. Science 127, 83–84. https://doi.org/10.1126/science.127.3289.83.

Haar, G. ter, 2010. Ultrasound bioeffects and safety. Proc. Inst. Mech. Eng. 224, 363–373. https://doi.org/10.1243/09544119JEIM613.

Jerusalem, A., Al-Rekabi, Z., Chen, H., Ercole, A., Malboubi, M., Tamayo-Elizalde, M., Verhagen, L., Contera, S., 2019. Electrophysiological-mechanical coupling in the neuronal membrane and its role in ultrasound neuromodulation and general anaesthesia. Acta Biomater. 97, 116–140. https://doi.org/10.1016/j.actbio.2019.07.041.

Kim, H., Chiu, A., Lee, S.D., Fischer, K., Yoo, S.-S., 2014. Focused ultrasound-mediated non-invasive brain stimulation: examination of sonication parameters. Brain Stimul. 7, 748–756. https://doi.org/10.1016/j.brs.2014.06.011.

Kim, H.-B., Swanberg, K.M., Han, H.-S., Kim, J.-C., Kim, J.-W., Lee, S., Lee, C.J., Maeng, S., Kim, T.-S., Park, J.-H., 2017. Prolonged stimulation with low-intensity ultrasound induces delayed increases in spontaneous hippocampal culture spiking activity: low-intensity ultrasound and hippocampal culture spiking. J. Neurosci. Res. 95, 885–896. https://doi.org/10.1002/jnr.23845.

King, R.L., Brown, J.R., Newsome, W.T., Pauly, K.B., 2013. Effective parameters for ultrasound-induced in vivo neurostimulation. Ultrasound Med. Biol. 39, 312–331. https://doi.org/10.1016/j.ultrasmedbio.2012.09.009.

Krasovitski, B., Frenkel, V., Shoham, S., Kimmel, E., 2011. Intramembrane cavitation as a unifying mechanism for ultrasound-induced bioeffects. Proc. Natl. Acad. Sci. 108, 3258–3263. https://doi.org/10.1073/pnas.1015771108.

Kubanek, J., Shi, J., Marsh, J., Chen, D., Deng, C., Cui, J., 2016. Ultrasound modulates ion channel currents. Sci. Rep. 6, 24170. https://doi.org/10.1038/srep24170.

Lai, C.-Y., Wu, C.-H., Chen, C.-C., Li, P.-C., 2006. Quantitative relations of acoustic inertial cavitation with sonoporation and cell viability. Ultrasound Med. Biol. 32, 1931–1941. https://doi.org/10.1016/j.ultrasmedbio.2006.06.020.

Legon, W., Bansal, P., Tyshynsky, R., Ai, L., Mueller, J.K., 2018. Transcranial focused ultrasound neuromodulation of the human primary motor cortex. Sci. Rep. 8, 10007. https://doi.org/10.1038/s41598-018-28320-1.

Liao, X., Walters, E.T., 2002. The use of elevated divalent cation solutions to isolate monosynaptic components of sensorimotor connections in Aplysia. J. Neurosci. Methods 120, 45–54.

Menz, M.D., Oralkan, O., Khuri-Yakub, P.T., Baccus, S.A., 2013. Precise neural stimulation in the retina using focused ultrasound. J. Neurosci. 33, 4550–4560. https://doi.org/10.1523/JNEUROSCI.3521-12.2013.

Newman, J., 2008. Sound. In: Physics of the Life Sciences. Springer New York, New York, NY, pp. 1–28. https://doi.org/10.1007/978-0-387-77259-2_11.

Plaksin, M., Shoham, S., Kimmel, E., 2014. Intramembrane cavitation as a predictive bio-piezoelectric mechanism for ultrasonic brain stimulation. Phys. Rev. X 4, 011004. https://doi.org/10.1103/PhysRevX.4.011004.

Prieto, M.L., Oralkan, Ö., Khuri-Yakub, B.T., Maduke, M.C., 2013. Dynamic response of model lipid membranes to ultrasonic radiation force. PLoS ONE 8, e77115. https://doi.org/10.1371/journal.pone.0077115.

Sakurai, A., Tamvacakis, A.N., Katz, P.S., 2016. Recruitment of polysynaptic connections underlies functional recovery of a neural circuit after lesion. ENeuro 3.

Tufail, Y., Yoshihiro, A., Pati, S., Li, M.M., Tyler, W.J., 2011. Ultrasonic neuromodulation by brain stimulation with transcranial ultrasound. Nat. Protoc. 6, 1453–1470. https://doi.org/10.1038/nprot.2011.371.

Vion-Bailly, J., N'Djin, W.A., Suarez Castellanos, I.M., Mestas, J.-L., Carpentier, A., Chapelon, J.-Y., 2019. A causal study of the phenomenon of ultrasound neurostimulation applied to an in vivo invertebrate nervous model. Sci. Rep. 9, 13738. https://doi.org/10.1038/s41598-019-50147-7.

Wang, B., Ke, W., Guang, J., Chen, G., Yin, L., Deng, S., He, Q., Liu, Y., He, T., Zheng, R., Jiang, Y., Zhang, Xiaoxue, Li, T., Luan, G., Lu, H.D., Zhang, M., Zhang, Xiaohui, Shu, Y., 2016. Firing frequency maxima of fast-spiking neurons in human, monkey, and mouse neocortex. Front. Cell. Neurosci. 10. https://doi.org/10.3389/fncel.2016.00239.

Wang, S., Meng, W., Ren, Z., Li, B., Zhu, T., Chen, H., Wang, Z., He, B., Zhao, D., Jiang, H., 2020. Ultrasonic neuromodulation and sonogenetics: a new era for neural modulation. Front. Physiol. 11, 787. https://doi.org/10.3389/fphys.2020.00787.

Wang, X., Yan, J., Wang, Z., Li, X., Yuan, Y., 2020. Neuromodulation effects of ultrasound stimulation under different parameters on mouse motor cortex. IEEE Trans. Biomed. Eng. 67, 291–297. https://doi.org/10.1109/TBME.2019.2912840.

Wright, C.J., Rothwell, J., Saffari, N., 2015. Ultrasonic stimulation of peripheral nervous tissue: an investigation into mechanisms. J. Phys. Conf. Ser. 581, 012003 https://doi.org/10.1088/1742-6596/581/1/012003.

Ye, P.P., Brown, J.R., Pauly, K.B., 2016. Frequency dependence of ultrasound neurostimulation in the mouse brain. Ultrasound Med. Biol. 42, 1512–1530. https://doi.org/10.1016/j.ultrasmedbio.2016.02.012.

Yoon, K., Lee, W., Lee, J.E., Xu, L., Croce, P., Foley, L., Yoo, S.-S., 2019. Effects of sonication parameters on transcranial focused ultrasound brain stimulation in an ovine model. PLOS ONE 14, e0224311. https://doi.org/10.1371/journal.pone.0224311.